SYNDOC: A HYBRID DISCRIMINATIVE-GENERATIVE FRAMEWORK FOR SYNTHETIC DOMAIN-ADAPTIVE DOCUMENT KEY INFORMATION EXTRACTION

Anonymous authors
Paper under double-blind review

ABSTRACT

Domain-specific Visually Rich Document Understanding (VRDU) presents significant challenges due to the complexity and sensitivity of documents in fields such as medicine, finance, and material science. Although existing Large (Multimodal) Language Models (LLMs/MLLMs) achieve promising results, they still suffer from hallucinations, limited domain adaptation, and heavy reliance on extensive fine-tuning datasets. We introduce SynDoc, a novel framework that combines discriminative and generative models to address these challenges. SynDoc features a robust synthetic data generation workflow that extracts structural information and generates domain-specific queries to produce high-quality annotations. Through adaptive instruction tuning, SynDoc improves the discriminative model's ability to extract domain-specific knowledge. In parallel, a recursive inference mechanism iteratively refines outputs from both models to achieve stable and accurate predictions. This integrated framework demonstrates scalable, efficient, and precise document understanding, bridging the gap between domain-specific adaptation and general world knowledge for key information extraction tasks.

1 INTRODUCTION

With the increasing demand for domain-specific Visually Rich Document Understanding (VRDU), significant opportunities are emerging across diverse areas such as medicine (Ding et al., 2023b), finance (Ding et al., 2023a), material science (Khalighinejad et al., 2024), and politics (Wang et al., 2023). These areas often rely on documents that contain extensive domain-specific knowledge and sensitive information, which pose unique challenges of key information extraction (KIE). As industries increasingly turn to AI-powered solutions for document analysis, the need for robust and adaptable frameworks to navigate these complexities has never been greater.

Vision-Language Pretrained Models (VLPMs) have demonstrated significant advancements in VRDU, typically in a **discriminative** manner by directly mapping multimodal inputs to key information through classification and sequence labeling (Huang et al., 2022; Gu et al., 2021; Lyu et al., 2024). Yet, these models encounter several challenges. First, they heavily depend on large-scale, domain-specific fine-tuning datasets (Ding et al., 2024a). Second, their performance often degrades in practical, zero-shot scenarios. In contrast, Multimodal Large Language Models (MLLMs) have recently been applied to extract key information from VRDs in a **generative** manner (OpenAI, 2024; Zhu et al., 2025), achieving remarkable progress due to their broad general knowledge; however, MLLMs still lack sufficient target-domain understanding, leading to unreliable or imprecise outputs in VRDU applications. For instance, as shown in Figure 1, an MLLM extracts the *present voting power* “18.86%" instead of the requested *previous voting power*, illustrating its limitations in understanding table structures.

Recent research has explored various strategies to address these challenges in document KIE, with synthetic data generation increasingly emerging as a crucial driver of progress for both discriminative and generative models (Wang et al., 2025; Xie et al., 2025; Tang et al., 2024). In the **discriminative** paradigm, domain-adaptive techniques applied to VLPM backbones have achieved promising results through fine-tuning on curated annotated datasets (Ding et al., 2024a). However, this approach remains constrained by high annotation costs and weak zero-shot performance. In contrast, **generative** models leverage synthetic data for self-supervised pretraining (Ye et al., 2023; Feng et al., 2024) and instruction tuning (Hu et al., 2024b; Zhang et al., 2025) to enhance multimodal VRD comprehension. Yet, these models face obstacles, including massive computational demands and suboptimal zero-shot performance when deployed in new domains. Moreover, synthetic data generated by MLLMs often suffers from low quality or inconsistency, particularly in question-answer pairs, leaving a gap in research on how to improve the trustworthiness of these synthetically generated instruction-response pairs (Ding et al., 2024b).

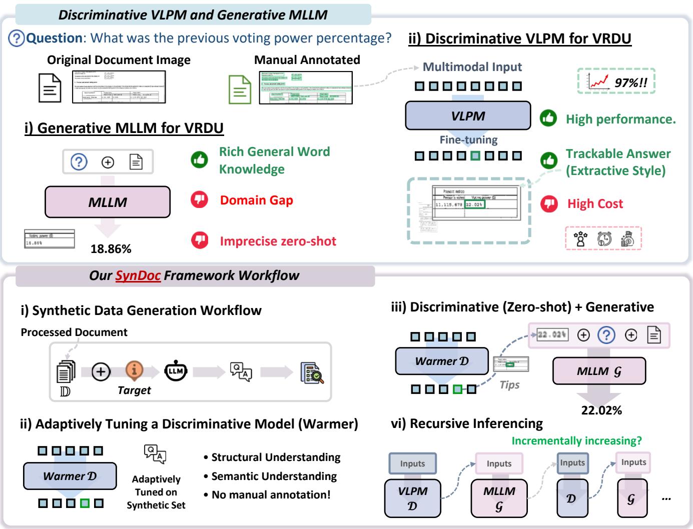
Discriminative VLPM and Generative MLLM
Question: What was the previous voting power percentage?
Original Document Image
Manual Annotated
i) Generative MLLM for VRDU
MLLM
18.86%
Rich General Word Knowledge
Domain Gap
Imprecise zero-shot
ii) Discriminative VLPM for VRDU
Multimodal Input
97%!!
VLPM
Fine-tuning
High performance.
Trackable Answer (Extractive Style)
High Cost
Our SynDoc Framework Workflow
i) Synthetic Data Generation Workflow
Processed Document
𝔻
Target
LLM
ii) Adaptively Tuning a Discriminative Model (Warmer)
Warmer 𝒟
Adaptively Tuned on Synthetic Set
• Structural Understanding
• Semantic Understanding
• No manual annotation!
iii) Discriminative (Zero-shot) + Generative
Warmer 𝒟
Tips
22.02%
MLLM 𝒢
22.02%
vi) Recursive Inferencing
Incrementally increasing?
Inputs
VLPM 𝒟
Inputs
MLLM 𝒢
Inputs
𝒟
Inputs
𝒢
...

Figure 1: Comparing SynDoc with discriminative and generative document KIE frameworks.

In this study, we propose SynDoc, a hybrid framework that introduces a new paradigm for document KIE by shifting from general-purpose LLM scaling to domain-specific adaptation tailored for concrete application scenarios. The contributions of this work are summarised as follows: ***First*, we shift the paradigm from general scaling to domain-focused scaling for specialized document KIE tasks.** We develop a synthetic data generation workflow that integrates OCR, PDF parsing, multi-task inquiry generation, and quality-verification modules. By applying the scaling law to the target domain, this pipeline produces large volumes of high-quality synthetic annotations that accurately capture both the structure and content of complex, domain-specific documents. ***Second*, we introduce the concept of a "warmer"—a lightweight discriminative retriever designed to adapt domain-specific knowledge and supply grounded multimodal cues to generative MLLMs.** By training only this efficient retriever rather than fine-tuning large MLLMs, the framework offers substantial computational savings and reduces dependence on large manually annotated datasets through synthetic data supervision. In addition, through iterative knowledge exchanging between warmer and MLLM, outputs from the discriminative and generative models are iteratively refined, yielding more context-aware, stable, and accurate zero-shot responses. ***Third*, we introduce domain adaptation strategies to train the joint-grained warmer, enabling it to bridge the gap between MLLM knowledge and target-domain documents.** Structural adaptation improves semantic–spatial understanding, while semantic adaptation strengthens user intent and content comprehension, both essential for strong zero-shot performance. After domain-adaptive tuning, the warmer can "warm up" domain knowledge for MLLM-based document KIE, enabling more accurate, contextually grounded inference. **Finally**, by integrating these components, SynDoc delivers a scalable and robust framework for domain-specific key information extraction, validated on three in-domain datasets and further tested for cross-domain generalization.

2 Related Work

Curated and synthetic data for VRDU Heuristic approaches (Watanabe et al., 1995; Seki et al., 2007) and statistical learning methods (Oliveira & Viana, 2017) have demonstrated strong performance in domain-specific document understanding. However, these methods rely heavily on expert effort, which limits their cross-domain adaptability. To address this limitation, recent advances employ self-supervised learning on large-scale, unannotated, and multi-source document collections (Huang et al., 2022; Tang et al., 2023; Lyu et al., 2024; Wang et al., 2022a; Hong et al., 2022; Harley et al., 2015), thereby improving generalizability and multimodal comprehension for broader VRDU tasks. When fine-tuned on curated datasets, these frameworks can achieve state-of-the-art performance in specific VRDU tasks. Yet, constructing such high-quality datasets is resource-intensive, hindering scalability and applicability to new document types (Jaume et al., 2019; Park et al., 2019; Ding et al., 2023b). To mitigate this bottleneck, recent research (Ding et al., 2024b) has explored using

LLMs/MLLMs to generate synthetic datasets with well-designed prompts and human verification. Other studies create large-scale synthetic datasets for self-supervised pretraining (Hu et al., 2024a; Feng et al., 2024) or instruct-tuning (Wang et al., 2025; Tang et al., 2024; Zhang et al., 2025) to enhance multimodal document understanding. For example, Ding et al. (2024a) pretrain VRDU models with synthetic QA pairs, followed by semi-supervised refinement, achieving performance comparable to full supervision. However, optimizing the quality of synthetic dataset generation and integrating SoTA MLLMs into real-world VRDU applications remains underexplored.

VRDU frameworks Self-supervised frameworks employ diverse pre-training tasks to enhance multimodal learning and achieve strong performance on downstream tasks when fine-tuned with curated datasets (Wang et al., 2022b; Appalaraju et al., 2023). However, most discriminative models rely heavily on off-the-shelf OCR tools, including the LayoutLM-series, making their extractive predictions vulnerable to errors and to propagation from both models and OCR systems (Huang et al., 2022; Xu et al., 2021). To address this vulnerability, end-to-end OCR-free frameworks have been developed to bypass OCR dependencies (Kim et al., 2022; Abramovich et al., 2024; Lyu et al., 2024). Nonetheless, these OCR-free models often operate with comparatively smaller parameters and limited training resources, which constrains their world knowledge and reduces generalization capacity without substantial annotations. By contrast, LLMs/MLLMs (OpenAI, 2024; Team et al., 2024; Laurençon et al., 2024; Yang et al., 2025) benefit from scaling laws and extensive training to capture broad world knowledge and support zero-shot or few-shot learning in VRD tasks (He et al., 2023). Despite these advantages, challenges such as hallucinations and limited domain-specific knowledge continue to undermine their reliability. To bridge this gap, our SynDoc introduces an adaptively tuned discriminative "warmer" that provides domain-specific knowledge to a generative MLLM. This integration enables recursive refinement of the inference process, combining domain-aware information and broad world knowledge to enhance the accuracy and reliability of key information extraction in VRDs.

3 Methods

3.1 Overview of SynDoc

Let $\mathbb{D}$ be a document collection within a *specific domain*. We introduce SynDoc, a hybrid framework designed to answer a user-provided natural language query q concerning a specific document $d \in \mathbb{D}$. SynDoc integrates a discriminative model $\mathcal{D}$ and a generative model $\mathcal{G}$ to address q in complementary extractive and abstractive manners, respectively. $\mathcal{D}$, termed **warmer**, employs pretrained backbones to capture target-domain knowledge, while $\mathcal{G}$ employs state-of-the-art LLM/MLLMs, guided by carefully designed prompts P, to generate answers in zero-shot scenarios.

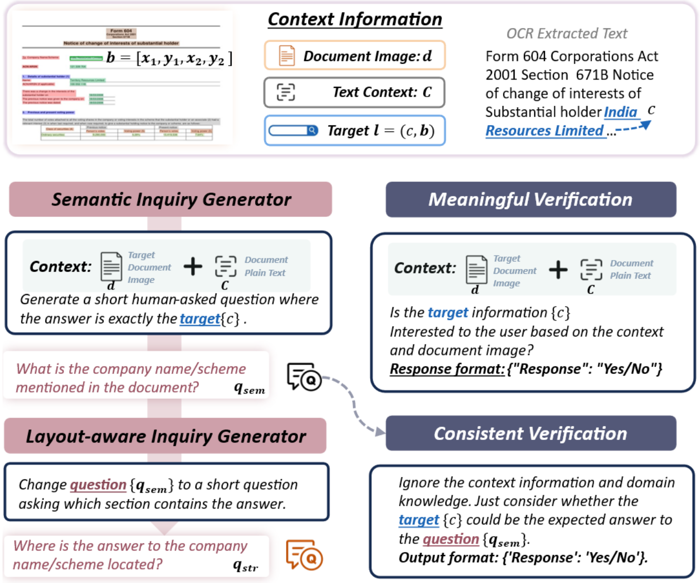

Generate a short human-asked question where the answer is exactly the target{c} .

What is the company name/scheme mentioned in the document? q_{sem}

Change question {q_{sem}} to a short question asking which section contains the answer.

Where is the answer to the company name/scheme located? q_{str}

Is the target information {c}
Interested to the user based on the context and document image?
Response format:{"Response": "Yes/No"}

Ignore the context information and domain knowledge. Just consider whether the target {c} could be the expected answer to the question {q_{sem}}.
Output format: {'Response': 'Yes/No'}.

Figure 2: Workflow of the Synthetic Data Generator.

To enable this workflow, we first construct the **synthetic datasets** (Figure 2). This process begins with the extraction of structural information using off-the-shelf tools (e.g., OCR or PDF parsers (Cui et al., 2025)). Next, domain-specific synthetic queries are generated with MLLMs, focusing separately on structural and content understanding. $\mathcal{D}$ incorporates multimodal representations, including textual, visual, layout, and structural features, alongside predictions from the MLLM.

During inference, the outputs from $\mathcal{D}$ and $\mathcal{G}$ undergo **iterative cross-feeding** until stable predictions are reached.

The following subsections detail the four key modules of SynDoc: (1) Synthetic Data Generator, (2) Discriminative Warmer Architecture, (3) Adaptive Instruction Tuning, and (4) Recursive Inference.

3.2 Synthetic Data Generator

VRD Structure Parsing We use off-the-shelf tools to extract both the **text content** and **layout structure** of a target document collection (Figure 2). For **document images**, we use a vision-based OCR system to extract text-line entities L. Each $l = (b, c) \in L$ includes a bounding box b and text content $c = \{\tau_i\}$, where each τ is a textual token. Bounding boxes are represented by coordinates $(x_{min}, y_{min}, x_{max}, y_{max})$. For **text-embedded PDF files**, we employ PDF parsing tools to acquire text-line or semantic entity sets L (e.g., paragraph, list, section), which provide more accurate structural information than OCR alone.

MLLM-driven Inquiry Generation For $\mathcal{D}$ to capture target-domain knowledge, we propose an MLLM-driven workflow with two modules (Figure 2). (1) **Multi-Task Inquiry Generation** produces diverse queries to instruction-tune $\mathcal{D}$ to enhance its structural and semantic understanding of the domain. Specifically, a set of text lines is randomly sampled and fed to an LLM to generate two types of QA pairs. First, *Semantic* QA pairs guide $\mathcal{D}$ to extract target information from a document. Given the content of a target entity along with its document and context information, the MLLM generates pairs (q_{sem}, c), where c is the answer to the generated question q_{sem}. Second, *Spatial-aware* QA pairs help $\mathcal{D}$ capture both semantic and spatial correlations. Here, each q_{sem} is transformed into a spatially-aware question q_{spt} by identifying the document region (e.g., top-left, top-middle, top-right) where the target information c is located. (2) **Multi-Aspect Quality Verification** is designed to filter out low-quality or noisy questions by assessing factors such as meaningfulness and question-answer consistency. This step ensures that synthetic QA pairs are both relevant and reliable for instruction-tuning $\mathcal{D}$. First, the process determines whether c is relevant to the end user (e.g., "Is c meaningful or interesting to the end user?"). Next, it verifies that c adequately addresses q_{sem} (e.g., "Could c reasonably serve as an answer to q_{sem}?").

3.3 Warmer Architecture

The **Warmer** ($\mathcal{D}$) utilizes a vision-language pre-trained model (VLPM) as its backbone, optimized for discriminative answer extraction through adaptively tuning on synthetic datasets (Figure 3). The adopted VLPM is pre-trained on layout-aware tasks and fine-tuned on well-annotated datasets, exhibiting strong performance on targeted VRDU tasks. To address zero-shot scenarios, the warmer architecture leverages the VLPM backbone to enable $\mathcal{D}$ to learn multi-aspect, domain-aware knowledge from synthetic datasets. In the following, we first introduce the initial feature representation used by $\mathcal{D}$ and then describe the detailed warmer architecture.

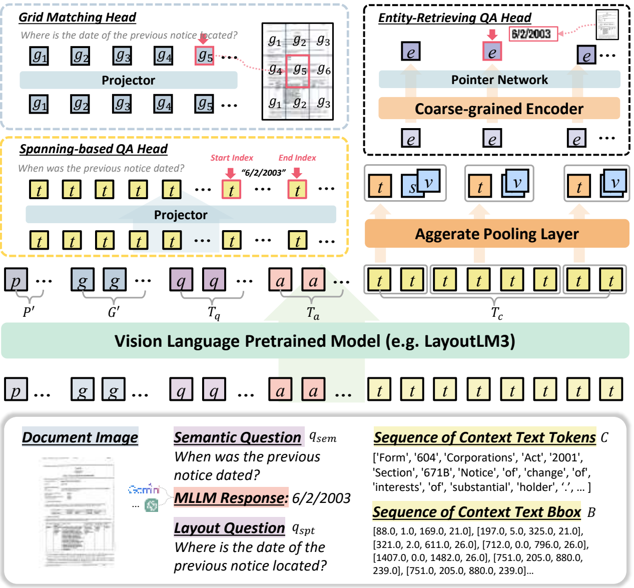
Grid Matching Head
Where is the date of the previous notice located?
g_1 g_2 g_3 g_4 g_5 …
Projector
g_1 g_2 g_3 g_4 g_5 g_6
Entity-Retrieving QA Head
6/2/2003
e
Pointer Network
Coarse-grained Encoder
Spanning-based QA Head
When was the previous notice dated?
Start Index
End Index
"6/2/2003"
t
Projector
s v
Aggerate Pooling Layer
p g q a t
P'
G'
T_q
T_a
T_c
Vision Language Pretrained Model (e.g. LayoutLM3)
Document Image
Semantic Question q_{sem}
MLLM Response: 6/2/2003
Layout Question q_{spt}
Sequence of Context Text Tokens C
Sequence of Context Text Bbox B

When was the previous notice dated?

Where is the date of the previous notice located?

['Form', '604', 'Corporations', 'Act', '2001', 'Section', '671B', 'Notice', 'of', 'change', 'of', 'interests', 'of', 'substantial', 'holder', '.', …]

[88.0, 1.0, 169.0, 21.0], [197.0, 5.0, 325.0, 21.0], [321.0, 2.0, 611.0, 26.0], [712.0, 0.0, 796.0, 26.0], [1407.0, 0.0, 1482.0, 26.0], [751.0, 205.0, 880.0, 239.0], [751.0, 205.0, 880.0, 239.0]…

Figure 3: Architecture of the discriminative Warmer.

Initial Feature Representation For a synthetically acquired entity set L from a document $d \in \mathbb{D}$, following Ding et al. (2024b), a vision pretrained model extracts visual representations v and a text pretrained model extracts textual sentence embedding s of any textline $l \in L$. A textual sequence $C = \{\tau_i\}_{i=1}^{n}$ represent textual context of target document d, combined with the projected bounding box $B = \{b_i\}_{i=1}^{n}$ and concatenated with document image patches P. For each semantic query q_{sem}, the MLLM-generated answer a can provide additional guidance for localization. Finally, grid embeddings $G = \{g_i\}_{i=1}^{j\times k}$ result from resizing and flattening the document image into a $j \times k$ grid, capturing global spatial layout information.

Detailed Architecture $\mathcal{D}$ processes the input sequence (q, a, C, P and B). These inputs are fed into a VLPM backbone $\mathcal{E}_w$ to derive embedded feature representations:

$$(P', G', T_q, T_a, T_c) = \mathcal{E}_w(P, G, q, a, C + B). \quad (1)$$

Here, T_q, T_a, and T_c denote the encoded textual features for the query, answer, and context, respectively, while P' and G' represent the encoded patch and grid features of the document image.

For each textline $l = (b, c) \in L$ extracted using parsing tools, a pooling layer aggregates the token features to obtain the entity-level representation e,

$$e = \text{Pooling}\big(\{\, \mathcal{E}_w(t_j) \mid t_j = \tau_j + b,\, \tau_j \in c \,\}\big) \oplus v \oplus s. \quad (2)$$

The enhanced entity features $E = \{e_l \mid l \in L\}$ are processed by an **Entity-Retrieval Head**, which includes a coarse-grained transformer encoder to improve entity-level contextual understanding and a pointer network to predict the final entity index (Ding et al., 2024b). Additionally, a fine-grained **Span-based QA Head** gets the encoded document text feature T_c to predict the start and end indices of the answer span for input query q. To enhance structural understanding within the target domain, a **Grid Matching Head** gets encoded grid embedding G' to predict the grid index of spatial-aware queries. Each of these heads may be trained at different stages to enable the Warmer to capture multi-aspect, domain-specific knowledge.

3.4 Adaptively Warmer Tuning

Step-by-step training enables the warmer $\mathcal{D}$ to effectively adapt to the target domain, starting with **structural adaptation** to enhance the domain-specific layout understanding, followed by **semantic adaptation** to locate target information based on the input query.

Structural Adaptation enhances both semantic and spatial comprehension by guiding $\mathcal{D}$ to identify the most relevant document grid $g' \in G'$ for a given structural query q_{str}. For example, given the query "*Where is the date of the previous notice located?*", $\mathcal{D}$ predicts the grid g_5 that contains the answer (Figure 3). A pointer network computes logits for each candidate grid (Ding et al., 2024b), and the probabilities are obtained using the softmax function. The structure adaptation loss is defined using cross-entropy:

$$\mathcal{L}_{str} = -\sum\nolimits_{g' \in G'} y_{g'} \log \hat{y}_{g'}, \quad (3)$$

where $y_{g'}$ represents the ground truth grid. This process ensures that $\mathcal{D}$ learns to associate structural queries with the correct document regions, improving retrieval accuracy and layout-aware reasoning.

Semantic Adaptation enables $\mathcal{D}$ to pretrain on a synthetic semantic QA set P, allowing it to understand document image I_d and q_{sem} for zero-shot extractive QA. The model employs two extractive QA heads. (1) *Fine-grained Span-based QA Head* predicts the start and end token indices using a linear projector. The cross-entropy loss is $\mathcal{L}_{fg} = -\sum_{t\in\mathcal{E}_w(c)} y_t^{\text{start}} \log \hat{y}_t^{\text{start}} + y_t^{\text{end}} \log \hat{y}_t^{\text{end}}$ where y_t^{start} and y_t^{end} denote the ground truth indices, and $\hat{y}_t^{\text{start}}$ and $\hat{y}_t^{\text{end}}$ are the predicted probabilities after softmax. (2) *Coarse-grained Entity-Retrieving Head* retrieves target entities based on entity logits and is optimized with a cross-entropy loss: $\mathcal{L}_{cg} = -\sum_{e\in E} y_e \log \hat{y}_e$ where y_e represents the ground truth distribution over the entity set E, and $\hat{y}_e$ is the predicted softmax probability. The final optimization objective combines both losses as:

$$\mathcal{L} = \lambda_{fg}\mathcal{L}_{fg} + \lambda_{cg}\mathcal{L}_{cg}, \quad (4)$$

where λ_{fg} and λ_{cg} balance the contributions of the fine-grained and coarse-grained QA losses. During semantic adaptation, different synthetic subsets may be selected based on *Multi-Aspect Quality Verification*, leading to potential variations in model performance, as described in Section 5.2.

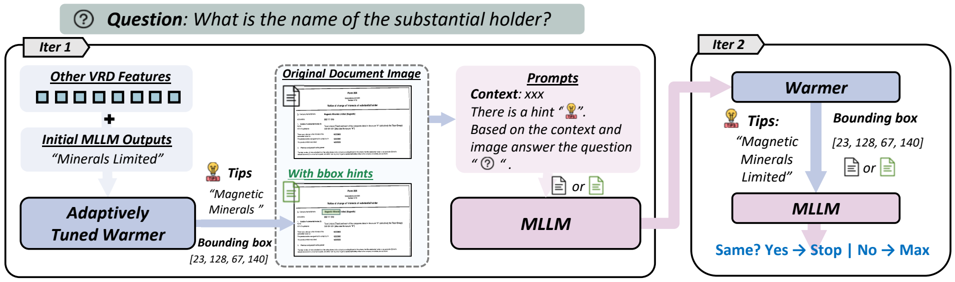

Figure 4: Recursive inference framework for zero-shot QA on VRDs. Given a query, the initial MLLM-generated answer is iteratively refined using retrieved entity hints ($L_{\mathcal{D}}$) retrieved by the adaptively tuned Warmer. Bounding-box cues and other VRD features guide the MLLM toward more accurate and context-aware answers in subsequent iterations.

3.5 Recursively Inferencing

We apply a **recursively inferencing strategy** to jointly leverage $\mathcal{D}$ and $\mathcal{G}$ for zero-shot question answering on VRDs (Figure 4). The top-k entities retrieved by $\mathcal{D}$, denoted $L_{\mathcal{D}}$, provide domain-specific guidance to enhance MLLM responses. Initially, given the prompt $(I_d, C, q_{sem}) \rightarrow \Pi$, $\mathcal{G}$ generates an answer $A_{\mathcal{G}}$. During the t-th recursive step, $\mathcal{D}$ updates its retrieval based on the previous $A_{\mathcal{G}}^{(t)}$, which in turn informs an updated prompt:

$$L_{\mathcal{D}}^{(t+1)} = \mathcal{D}(A_{\mathcal{G}}^{(t)}), \quad \Pi^{(t+1)} = \text{UpdatePrompt}(\Pi^{(t)}, L_{\mathcal{D}}^{(t+1)}), \quad A_{\mathcal{G}}^{(t+1)} = \mathcal{G}(\Pi^{(t+1)}). \tag{5}$$

This iterative process allows $\mathcal{G}$ to progressively incorporate domain-specific knowledge, improving the accuracy and reliability of its answers. Recursive inference continues until a maximum recursion depth is reached or the generated answer stabilizes. Through this approach, both extractive and generative outputs are iteratively refined.

4 Experimental Settings

4.1 Datasets

We evaluated SynDoc on four domain-specific document KIE datasets: FormNLU (financial forms) (Ding et al., 2023a), CORD (receipts) (Park et al., 2019), Ephoie (exam papers) (Wang et al., 2021), and FUNSD (Jaume et al., 2019) (multi-domains) (Appendix A.1 for more details). Form-NLU is further divided into Printed (F-P) and Handwritten (F-H) subsets. For each *test set*, document images were processed using the *Synthetic Data Generation* module to produce synthetic structural annotations and QA pairs with quality verification. During inference, the original QA pairs or key-value/question pairs are used to evaluate performance.

For the FUNSD and CORD datasets, we utilized the processed test sets from Luo et al. (2024). For Form-NLU and Ephoie, key-value pairs were converted into QA pairs for inference. Following prior works (Mathew et al., 2021; Luo et al., 2024), we adopted the Averaged Normalized Levenshtein Similarity (ANLS) as the primary **evaluation metric**.

4.2 Baselines and Implementation Details

We evaluated SynDoc against a range of SoTA baselines, including open-source models (Qwen2-VL (Wang et al., 2024), Idefics2 (Laurençon et al., 2024), InternVL2 (Chen et al., 2024)) and proprietary systems (GPT-4o (OpenAI, 2024), Gemini 1.5 (Team et al., 2024)). These models were selected for their demonstrated effectiveness in document-centric tasks, including comprehension, retrieval, and question answering. For consistency, all MLLMs were assessed under default inference settings in the HuggingFace environment using up to 2× A100 80G GPUs. Warmer tuning employed a batch size of 16, a learning rate of $2e{-}5$, and the AdamW optimizer.

5 Results and Discussion

5.1 Main Results

Table 1 shows that proprietary models generally outperform their open-source counterparts, with the gap most pronounced in complex scenarios (e.g., F-H and Ephoie). Among open-source MLLMs of similar size, Qwen2-VL achieves the highest performance, likely due to its extensive multimodal training data and advanced OCR capabilities. Intern-VL2 also performs consistently well across all datasets, whereas Idefics2 struggles with structurally complex documents, particularly in Ephoie.

Table 1: Zero-shot MLLM results. The last row shows the best configuration with bounding boxes.

Model	F-P	F-H	CORD	Ephoie	FUNSD
Idefics2	57.54	33.31	54.45	15.22	62.11
InternVL2	66.56	45.47	66.84	68.92	74.95
Qwen2-VL	78.05	43.65	77.86	70.36	79.12
GPT-4o	76.16	56.49	79.05	79.40	80.05
Gemini	76.09	66.86	84.35	81.82	83.56
SynDoc (Gemini)					
Top-1	80.29	67.73	85.19	81.80	82.77
Top-K	81.60	66.90	83.57	81.33	82.12
Top-1 R	80.29	67.73	85.19	**82.15**	83.02
Top-K R	**81.91**	68.09	84.57	81.58	82.40
w/bbox	80.93	**68.13**	**85.40**	82.08	**83.87**

Since Gemini shows superior performance across most benchmark datasets compared to GPT-4o, we present the results of the Gemini-based SynDoc framework. Overall, incorporating adaptively tuned warmer knowledge into MLLMs enhances performance on domain-specific datasets; however, it can introduce noise in cross-domain benchmarks such as FUNSD. The results also suggest that employing top-K candidate hints or applying recursive inference (top-K R) substantially improves MLLM performance in zero-shot scenarios.

5.2 Warmer Performance Analysis

Here, we evaluated the effectiveness of the *Synthetic Data Generation* workflow and *Warmer*'s ability to capture domain-specific knowledge in three aspects: adaptive tuning strategies, top-k entity retrieval variations, and different pre-trained backbones. These experiments aim to determine whether the proposed methods optimize Warmer's performance and enhance information extraction in zero-shot scenarios, thereby providing strong support for downstream MLLM inference. Notably, Table 2 shows that, without tuning on synthetically generated data, the pre-trained Warmer failed to retrieve any meaningful information from the target document context.

Table 2: Results under various Warmer adaptive tuning settings. Adapt denotes 4 configurations: (1) full synthetic set, (2) meaningfulness verification subset, (3) consistency verification subset, and (4) both subsets. St - structure adaptation. Prior - prior MLLM outputs.

Adapt	St	Prior	F-P	F-H	CORD	**Ephoie**	FUNSD
N/A	✗	✗	0	0	0	0	0
1	✗	✗	31.39	18.18	41.48	19.23	44.37
2	✗	✗	42.56	16.41	46.71	20.64	48.66
3	✗	✗	33.87	14.61	41.16	22.74	42.77
4	✗	✗	44.23	12.23	50.44	23.78	44.67
1	✗	✓	59.26	30.67	65.60	22.94	56.83
2	✗	✓	65.67	31.63	66.37	22.06	57.77
3	✗	✓	64.68	27.85	65.9	25.48	57.43
4	✗	✓	65.75	29.31	65.08	24.76	59.86
1	✓	✓	62.67	30.25	66.21	24.12	58.08
2	✓	✓	66.03	**31.64**	**67.26**	24.13	58.05
3	✓	✓	65.2	28.83	63.94	25.29	61.01
4	✓	✓	**66.19**	28.29	66.25	**27.16**	**61.24**

Adaptive Tuning Strategies We first evaluated the Warmer's performance under different adaptive tuning methods in adaptive tuning sets, prior MLLM outputs, and structural-adaptive tuning.

i) *Effects of adaptive tuning sets.* Table 2 shows that both verification methods improve performance and enhance domain adaptation. In particular, meaningfulness verification consistently boosts performance, whereas consistency verification occasionally has a negative impact, likely because OCR errors lead to inaccurate MLLM justifications.

ii) *Impact of prior MLLM outputs.* Table 2 shows that incorporating MLLM outputs as Warmer input further improves its ability to locate relevant information. For instance, ANLS increased from 41.48 to 66.37 on CORD, 44.37 to 61.24 on FUNSD, and 19.23 to 27.16 on Ephoie. While the synthetic dataset remains the primary source of the Warmer's knowledge, providing MLLM inputs helps it efficiently locate target answers.

iii) *Structural Adaption Tuning.* This mechanism enhances the Warmer's comprehension of layout and semantic correlations within a specific domain. Table 2 demonstrates consistent improvements across datasets: CORD increasing from 50.44 to 67.26, FUNSD from 44.67 to 61.24, and Ephoie from 22.74 to 27.16, when comparing the best results with and without structural adaptation. These result indicates that self-supervised structural adaptation effectively warms up the Warmer, enabling richer structural and semantic representations and enhancing subsequent semantic adaptation.

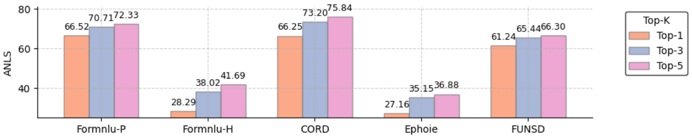

Figure 5: Top-K retrieved entity performance using LayoutLMv3.

Top-K Retrieved Entity Performance While the Warmer's maximum likelihood prediction may not always yield the most relevant result, leveraging Top-K likelihood predictions can enhance the MLLM's ability to locate the correct answer (Section 5.1). We compared Top-1, Top-3, and Top-5 retrieved entities, selecting the entity with the highest ANLS when multiple candidates are available.

Figure 5 shows that the Top-3 predictions significantly improve the retrieval of relevant information compared to Top-1. However, the gain from Top-3 to Top-5 is marginal. Notably, the improvement from Top-1 to Top-3 is especially pronounced for datasets with lower OCR accuracy, indicating the benefit of broader retrieval in error-prone scenarios.

Various Warmer Backbones We selected three commonly used pretrained backbones to assess their effectiveness: the text-only RoBERTa (Liu, 2019), the text-and-layout-aware LiLT (Wang et al., 2022a), and the text, layout, and vision-aware LayoutLMv3 (Huang et al., 2022). Table 3 shows that multimodal frameworks tend to outperform the monomodal RoBERTa, particularly when OCR errors impact the input text. However, LayoutLMv3 exhibits weaker feature representations, significantly underperforming LiLT and RoBERTa despite all three using the same xlm-RoBERTa-base checkpoints. Interestingly, there are instances where the monomodal RoBERTa outperforms multimodal backbones, indicating that multimodal architectures do not always guarantee superior performance or enhanced domain-specific knowledge extraction.

Table 3: Comparison of results under different Warmer backbone configurations.

Model	F-P	F-H	CORD	Ephoie	FUNSD
Roberta	64.18	23.85	**70.40**	31.57	59.44
LiLT	63.82	30.89	67.87	**31.97**	**60.94**
LayoutLMv3	**65.75**	**31.63**	66.37	25.48	59.86

5.3 Ablation Studies

Here, we assessed the effectiveness of the zero-shot trained Warmer for enhancing MLLM inference and explored the impact of the recursive inference mechanism across various MLLMs.

Performance on Various MLLMs Table 4 reports the results for two high-performing open-source models (InternVL and QWenVL) alongside the best-performing proprietary model (Gemini). Across all models and datasets, incorporating Warmer outputs consistently improves performance, suggesting that the Warmer successfully captures task-specific patterns that generic MLLMs might overlook.

Table 4: Comparison of Warmer to Generative Models.

	F-P		F-H		CORD		Ephoie	
Model	Vani.	Ours	Vani.	Ours	Vani.	Ours	Vani.	Ours
InternVL	66.56	↑ 68.09	45.47	↑ 46.81	66.84	↑ 68.80	68.92	↑ 70.29
QWenVL	78.05	↓ 77.27	43.65	↑ 44.43	77.86	↑ 78.44	70.36	↑ 75.03
Gemini	76.09	↑ 81.91	66.86	↑ 68.02	84.35	↑ 85.19	81.82	↑ 82.15

Recursive Warmer Performance Table 5 shows that recursive inference enhances the performance of both discriminative Warmer and generative MLLM. Notably, the FormNLU dataset exhibits substantial gains, with scores rising from 66.19 to 73.76 on the printed subset and from 31.64 to 39.15 on the handwritten subset. Interestingly, the peak performance of Warmer and MLLM does not always coincide at the same iteration. This suggests that, while Warmer steadily improves retrieval quality, Gemini might require

Table 5: Impact of iteration count on Warmer and Gemini.

	F-P		F-H		CORD		Ephoie	
	Warmer	Gemini	Warmer	Gemini	Warmer	Gemini	Warmer	Gemini
N/A	66.19	76.09	31.64	66.86	**67.26**	84.35	27.16	81.82
1	73.57	**80.29**	38.11	**67.73**	63.37	**85.19**	**27.98**	81.80
2	**73.76**	80.17	38.79	67.60	64.15	84.67	25.94	81.91
3	73.72	80.15	**39.15**	67.32	64.32	84.65	26.03	81.71
4	73.76	79.88	38.84	67.63	64.32	84.39	25.94	**82.15**
5	73.60	80.06	38.92	67.63	64.04	84.40	26.12	81.86

additional iterations to fully leverage these improvements during its integration and reasoning process.

Effectiveness of Top-K Candidates Figure 6 shows that providing top-K candidates from the Warmer can increase the likelihood of integrating relevant extracted information into MLLMs and improve performance. For instance, in FormNLU, retrieving additional information from the Warmer help guide Gemini to focus on the relevant context, thereby enhancing its performance. However, this approach also carries the risk of incorporating noise into the prompt, which may negatively impact the generative model's performance. This effect is particularly notable in InternVL2 and QWenVL2 when applied to OCR-challenging datasets, such as F-H and Ephoie.

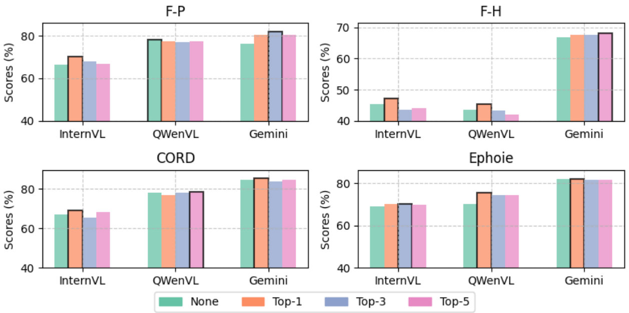

Figure 6: Result comparison by feeding Top-K Warmer-Retrieved Candidates into MLLM.

6 Case Study

To further illustrate the effectiveness of SynDoc, Figure 7 presents several examples where initial MLLM predictions are refined using SynDoc. Additional examples are provided in Appendix F. In ***Q1***, a question regarding the present voting count initially yields an incorrect answer of "15,41", which is subsequently corrected to "27,210" with the aid of the Warmer. This example highlights how the Warmer injects domain-specific knowledge, mitigating hallucinations and reducing the imprecision of MLLM predictions. Relying solely on the Top-1 retrieved answer from the Warmer, however, may not always capture the most relevant context for accurate answering. As demonstrated in ***Q2***, providing Top-3 entities allows the model to leverage both the Warmer's domain-specific knowledge and the MLLM's general world knowledge, thereby refining the final prediction. Finally, ***Q3*** showcases the iterative inference mechanism. Here, the Warmer and MLLM improve each other's outputs, leading to an almost correct prediction. Notably, even when the Warmer provides the ideal hints in the final iteration, OCR errors may persist. However, the MLLM compensates for these issues by leveraging its extensive general knowledge to make accurate predictions.

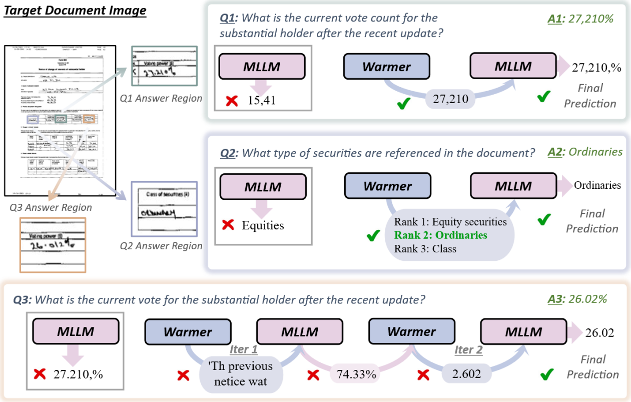

Figure 7: Qualitative Case Studies for Q1) Effectiveness of Warmer Retrieving; Q2) Demonstrating the Top-K candidates; 3) Effectiveness of iterative Inferencing.

7 Conclusion

In this paper, we introduced SynDoc, a novel VRDU framework that seamlessly integrates discriminative VLPMs with generative MLLMs to advance domain-specific VRDU performance, particularly in zero-shot settings. Our extensive experiments show that the proposed *Synthetic Data Generator* and *Adaptive Warmer Tuning* enable the discriminative Warmer to efficiently acquire domain knowledge and, together with recursive inference, drive continual performance gains for both the warmer and the MLLM. While SynDoc exhibits strong results across multiple domain-specific datasets, further work may be needed to enhance its generalizability and robustness in cross-domain applications.

Ethics Statement

This work adheres to the ICLR Code of Ethics. In this study, no human subjects or animal experimentation were involved. All datasets used were sourced in compliance with relevant usage guidelines, ensuring no privacy violations. We have taken care to avoid any biases or discriminatory outcomes in our research process. No personally identifiable information was used, and no experiments were conducted that could raise privacy or security concerns. We are committed to maintaining transparency and integrity throughout the research process.

Reproducibility Statement

We have made every effort to ensure that the results presented in this paper are reproducible. All code and models will be made publicly available upon acceptance to enable verification and replication. As detailed in Section 4.2, our experimental setup is fully specified, including the training procedure, model architecture, and computational environment.

Additionally, all datasets used are publicly accessible, ensuring consistency in our evaluation. We believe these measures will enable other researchers to reproduce our work and further advance the field.

References

Ofir Abramovich, Niv Nayman, Sharon Fogel, Inbal Lavi, Ron Litman, Shahar Tsiper, Royee Tichauer, Srikar Appalaraju, Shai Mazor, and R Manmatha. Visfocus: Prompt-guided vision encoders for ocr-free dense document understanding. In *European Conference on Computer Vision*, pp. 241–259. Springer, 2024.

Srikar Appalaraju, Peng Tang, Qi Dong, Nishant Sankaran, Yichu Zhou, and R Manmatha. Docformerv2: Local features for document understanding. *arXiv preprint arXiv:2306.01733*, 2023.

Zhe Chen, Jiannan Wu, Wenhai Wang, Weijie Su, Guo Chen, Sen Xing, Muyan Zhong, Qinglong Zhang, Xizhou Zhu, Lewei Lu, et al. Internvl: Scaling up vision foundation models and aligning for generic visual-linguistic tasks. In *Proceedings of the IEEE/CVF Conference on Computer Vision and Pattern Recognition*, pp. 24185–24198, 2024.

Cheng Cui, Ting Sun, Suyin Liang, Tingquan Gao, Zelun Zhang, Jiaxuan Liu, Xueqing Wang, Changda Zhou, Hongen Liu, Manhui Lin, Yue Zhang, Yubo Zhang, Handong Zheng, Jing Zhang, Jun Zhang, Yi Liu, Dianhai Yu, and Yanjun Ma. Paddleocr-vl: Boosting multilingual document parsing via a 0.9b ultra-compact vision-language model, 2025. URL `https://arxiv.org/abs/2510.14528`.

Yihao Ding, Siqu Long, Jiabin Huang, Kaixuan Ren, Xingxiang Luo, Hyunsuk Chung, and Soyeon Caren Han. Form-nlu: Dataset for the form natural language understanding. In *Proceedings of the 46th International ACM SIGIR Conference on Research and Development in Information Retrieval*, pp. 2807–2816, 2023a.

Yihao Ding, Siwen Luo, Hyunsuk Chung, and Soyeon Caren Han. Pdf-vqa: A new dataset for real-world vqa on pdf documents. In *Machine Learning and Knowledge Discovery in Databases: Applied Data Science and Demo Track*, pp. 585–601. Springer Nature Switzerland, 2023b.

Yihao Ding, Soyeon Caren Han, Zechuan Li, and Hyunsuk Chung. David: Domain adaptive visually-rich document understanding with synthetic insights. *arXiv preprint arXiv:2410.01609*, 2024a.

Yihao Ding, Kaixuan Ren, Jiabin Huang, Siwen Luo, and Soyeon Caren Han. Mmvqa: A comprehensive dataset for investigating multipage multimodal information retrieval in pdf-based visual question answering. In *Proceedings of the Thirty-Third International Joint Conference on Artificial Intelligence, IJCAI*, pp. 3–9, 2024b.

Hao Feng, Qi Liu, Hao Liu, Jingqun Tang, Wengang Zhou, Houqiang Li, and Can Huang. Docpedia: Unleashing the power of large multimodal model in the frequency domain for versatile document understanding. *Science China Information Sciences*, 67(12):1–14, 2024.

Jiuxiang Gu, Jason Kuen, Vlad I Morariu, Handong Zhao, Rajiv Jain, Nikolaos Barmpalios, Ani Nenkova, and Tong Sun. Unidoc: Unified pretraining framework for document understanding. *Advances in Neural Information Processing Systems*, 34:39–50, 2021.

Adam W Harley, Alex Ufkes, and Konstantinos G Derpanis. Evaluation of deep convolutional nets for document image classification and retrieval. In *2015 13th International Conference on Document Analysis and Recognition (ICDAR)*, pp. 991–995. IEEE, 2015.

Jiabang He, Lei Wang, Yi Hu, Ning Liu, Hui Liu, Xing Xu, and Heng Tao Shen. Icl-d3ie: In-context learning with diverse demonstrations updating for document information extraction. In *Proceedings of the IEEE/CVF International Conference on Computer Vision*, pp. 19485–19494, 2023.

Teakgyu Hong, Donghyun Kim, Mingi Ji, Wonseok Hwang, Daehyun Nam, and Sungrae Park. Bros: A pre-trained language model focusing on text and layout for better key information extraction from documents. In *Proceedings of the AAAI Conference on Artificial Intelligence*, volume 36, pp. 10767–10775, 2022.

Anwen Hu, Haiyang Xu, Jiabo Ye, Ming Yan, Liang Zhang, Bo Zhang, Ji Zhang, Qin Jin, Fei Huang, and Jingren Zhou. mplug-docowl 1.5: Unified structure learning for ocr-free document understanding. In *Findings of the Association for Computational Linguistics: EMNLP 2024*, pp. 3096–3120, 2024a. URL https://aclanthology.org/2024.findings-emnlp.175.

Anwen Hu, Haiyang Xu, Liang Zhang, Jiabo Ye, Ming Yan, Ji Zhang, Qin Jin, Fei Huang, and Jingren Zhou. mplug-docowl2: High-resolution compressing for ocr-free multi-page document understanding. *CoRR*, 2024b.

Yupan Huang, Tengchao Lv, Lei Cui, Yutong Lu, and Furu Wei. Layoutlmv3: Pre-training for document ai with unified text and image masking. In *Proceedings of the 30th ACM International Conference on Multimedia*, pp. 4083–4091, 2022.

Guillaume Jaume, Hazim Kemal Ekenel, and Jean-Philippe Thiran. Funsd: A dataset for form understanding in noisy scanned documents. In *2019 International Conference on Document Analysis and Recognition Workshops (ICDARW)*, volume 2, pp. 1–6. IEEE, 2019.

Ghazal Khalighinejad, Sharon Scott, Ollie Liu, Kelly L Anderson, Rickard Stureborg, Aman Tyagi, and Bhuwan Dhingra. Matvix: Multimodal information extraction from visually rich articles. *arXiv preprint arXiv:2410.20494*, 2024.

Geewook Kim, Teakgyu Hong, Moonbin Yim, JeongYeon Nam, Jinyoung Park, Jinyeong Yim, Wonseok Hwang, Sangdoo Yun, Dongyoon Han, and Seunghyun Park. Ocr-free document understanding transformer. In *Computer Vision–ECCV 2022: 17th European Conference, Tel Aviv, Israel, October 23–27, 2022, Proceedings, Part XXVIII*, pp. 498–517. Springer, 2022.

Hugo Laurençon, Léo Tronchon, Matthieu Cord, and Victor Sanh. What matters when building vision-language models?, 2024. URL https://arxiv.org/abs/2405.02246.

Yinhan Liu. Roberta: A robustly optimized bert pretraining approach. *arXiv preprint arXiv:1907.11692*, 364, 2019.

Chuwei Luo, Yufan Shen, Zhaoqing Zhu, Qi Zheng, Zhi Yu, and Cong Yao. Layoutllm: Layout instruction tuning with large language models for document understanding. *arXiv preprint arXiv:2404.05225*, 2024.

Pengyuan Lyu, Yulin Li, Hao Zhou, Weihong Ma, Xingyu Wan, Qunyi Xie, Liang Wu, Chengquan Zhang, Kun Yao, Errui Ding, et al. Structextv3: An efficient vision-language model for text-rich image perception, comprehension, and beyond. *arXiv preprint arXiv:2405.21013*, 2024.

Minesh Mathew, Dimosthenis Karatzas, and CV Jawahar. Docvqa: A dataset for vqa on document images. In *Proceedings of the IEEE/CVF winter conference on applications of computer vision*, pp. 2200–2209, 2021.

Dario Augusto Borges Oliveira and Matheus Palhares Viana. Fast cnn-based document layout analysis. In *2017 IEEE International Conference on Computer Vision Workshops (ICCVW)*, pp. 1173–1180. IEEE, 2017.

OpenAI. Hello gpt-4o. https://openai.com/index/hello-gpt-4o/, 2024.

Seunghyun Park, Seung Shin, Bado Lee, Junyeop Lee, Jaeheung Surh, Minjoon Seo, and Hwalsuk Lee. Cord: a consolidated receipt dataset for post-ocr parsing. In *Workshop on Document Intelligence at NeurIPS 2019*, 2019.

Minenobu Seki, Masakazu Fujio, Takeshi Nagasaki, Hiroshi Shinjo, and Katsumi Marukawa. Information management system using structure analysis of paper/electronic documents and its applications. In *Ninth International Conference on Document Analysis and Recognition (ICDAR 2007)*, volume 2, pp. 689–693. IEEE, 2007.

Jingqun Tang, Chunhui Lin, Zhen Zhao, Shu Wei, Binghong Wu, Qi Liu, Hao Feng, Yang Li, Siqi Wang, Lei Liao, et al. Textsquare: Scaling up text-centric visual instruction tuning. *arXiv preprint arXiv:2404.12803*, 2024.

Zineng Tang, Ziyi Yang, Guoxin Wang, Yuwei Fang, Yang Liu, Chenguang Zhu, Michael Zeng, Cha Zhang, and Mohit Bansal. Unifying vision, text, and layout for universal document processing. In *Proceedings of the IEEE/CVF Conference on Computer Vision and Pattern Recognition*, pp. 19254–19264, 2023.

Gemini Team, Petko Georgiev, Ving Ian Lei, Ryan Burnell, Libin Bai, and et al. Gemini 1.5: Unlocking multimodal understanding across millions of tokens of context, 2024. URL https://arxiv.org/abs/2403.05530.

Jiapeng Wang, Chongyu Liu, Lianwen Jin, Guozhi Tang, Jiaxin Zhang, Shuaitao Zhang, Qianying Wang, Yaqiang Wu, and Mingxiang Cai. Towards robust visual information extraction in real world: New dataset and novel solution. In *Proceedings of the AAAI Conference on Artificial Intelligence*, volume 35, pp. 2738–2745, 2021.

Jiapeng Wang, Lianwen Jin, and Kai Ding. Lilt: A simple yet effective language-independent layout transformer for structured document understanding. In *Proceedings of the 60th Annual Meeting of the Association for Computational Linguistics (Volume 1: Long Papers)*, pp. 7747–7757, 2022a.

Peng Wang, Shuai Bai, Sinan Tan, Shijie Wang, Zhihao Fan, Jinze Bai, Keqin Chen, Xuejing Liu, Jialin Wang, Wenbin Ge, Yang Fan, Kai Dang, Mengfei Du, Xuancheng Ren, Rui Men, Dayiheng Liu, Chang Zhou, Jingren Zhou, and Junyang Lin. Qwen2-vl: Enhancing vision-language model's perception of the world at any resolution. *arXiv preprint arXiv:2409.12191*, 2024.

Wenjin Wang, Zhengjie Huang, Bin Luo, Qianglong Chen, Qiming Peng, Yinxu Pan, Weichong Yin, Shikun Feng, Yu Sun, Dianhai Yu, et al. Ernie-mmlayout: Multi-grained multimodal transformer for document understanding. *arXiv preprint arXiv:2209.08569*, 2022b.

Zilong Wang, Yichao Zhou, Wei Wei, Chen-Yu Lee, and Sandeep Tata. Vrdu: A benchmark for visually-rich document understanding. In *Proceedings of the 29th ACM SIGKDD Conference on Knowledge Discovery and Data Mining*, pp. 5184–5193, 2023.

Zining Wang, Tongkun Guan, Pei Fu, Chen Duan, Qianyi Jiang, Zhentao Guo, Shan Guo, Junfeng Luo, Wei Shen, and Xiaokang Yang. Marten: Visual question answering with mask generation for multi-modal document understanding, 2025. URL https://arxiv.org/abs/2503.14140.

Toyohide Watanabe, Qin Luo, and Noboru Sugie. Layout recognition of multi-kinds of table-form documents. *IEEE Transactions on Pattern Analysis and Machine Intelligence*, 17(4):432–445, 1995.

Xudong Xie, Hao Yan, Liang Yin, Yang Liu, Jing Ding, Minghui Liao, Yuliang Liu, Wei Chen, and Xiang Bai. Pdf-wukong: A large multimodal model for efficient long pdf reading with end-to-end sparse sampling, 2025. URL https://arxiv.org/abs/2410.05970.

Yiheng Xu, Tengchao Lv, Lei Cui, Guoxin Wang, Yijuan Lu, Dinei Florencio, Cha Zhang, and Furu Wei. Layoutxlm: Multimodal pre-training for multilingual visually-rich document understanding. *arXiv preprint arXiv:2104.08836*, 2021.

An Yang, Anfeng Li, Baosong Yang, Beichen Zhang, Binyuan Hui, Bo Zheng, Bowen Yu, Chang Gao, Chengen Huang, Chenxu Lv, et al. Qwen3 technical report. *arXiv preprint arXiv:2505.09388*, 2025.

Jiabo Ye, Anwen Hu, Haiyang Xu, Qinghao Ye, Ming Yan, Yuhao Dan, Chenlin Zhao, Guohai Xu, Chenliang Li, Junfeng Tian, Qian Qi, Ji Zhang, and Fei Huang. mplug-docowl: Modularized multimodal large language model for document understanding, 2023. URL https://arxiv.org/abs/2307.02499.

Jiaxin Zhang, Wentao Yang, Songxuan Lai, Zecheng Xie, and Lianwen Jin. Dockylin: A large multimodal model for visual document understanding with efficient visual slimming. In *Proceedings of the AAAI Conference on Artificial Intelligence*, volume 39, pp. 9923–9932, 2025.

Zhaoqing Zhu, Chuwei Luo, Zirui Shao, Feiyu Gao, Hangdi Xing, Qi Zheng, and Ji Zhang. A simple yet effective layout token in large language models for document understanding. *arXiv preprint arXiv:2503.18434*, 2025. URL https://arxiv.org/abs/2503.18434.

A DETAILED DATASET INFORMATION

A.1 DATASET DESCRIPTION

Table S1 summarizes the datasets used in this study.

Form-NLU is introduced for financial-domain form layout and content understanding, focusing on single-template, multi-format forms across digital, printed, and handwritten variations (Ding et al., 2023a). This dataset specifically addresses KIE tasks, which involve extracting 12 types of key information from more challenging printed and handwritten documents. Examples of these key information fields include "*Substantial Holder Name*", "*Previous Persons' Votes*", and others.

CORD is proposed for receipt understanding with diverse receipt templates (Park et al., 2019). This dataset focuses on the KIE sub-task of extracting fine-grained key information from scanned receipts, such as "*store name*" and "*item quantity*".

Ephoie is a dataset designed to understand scanned Chinese exam paper headers (Wang et al., 2021). The collected exam papers have diverse templates and handwritten information. This dataset focuses on the KIE sub-task to extract information from these exam papers, such as "*Score*," "*School*," and "*Student Name*."

FUNSD is a dataset for form understanding, comprising scanned form images from diverse sources with varying templates (Jaume et al., 2019). Each form contains predefined key-value pairs categorized as "*Question*" and "*Answer*" in the metadata. This dataset is used to assess the proposed framework's ability to handle cross-domain scenarios.

Table S1: Dataset statistics across different datasets, including the size of the original test and the synthetic dataset.

Domain	**Category**	**# Doc**	**# QA**	**Set 1**	**Set 2**	**Set 3**	**Set 4**
FormNLU-P	Financial Form	50	596	1937	1137	1073	676
FormNLU-H	Financial Form	50	597	1998	621	815	302
CORD	Receipt	100	156	1644	1535	988	968
EPHOIE	Exam Paper	311	928	2488	1746	1553	1159
FUNSD	Cross-domain	50	467	2036	1905	1088	1022

B Detailed Model Information

Table S2 summarizes baseline models for visual-rich document understanding.

Table S2: Baseline Models for Visual-rich Document Understanding.

Model	Params	Modality	Training Data	Status
RoBERTa	125M	Text	Web, Books	Open
LiLT	131M	Text+Layout	IIT-CDIP	Open
LayoutLMv3	133M	Text+Layout+Vision	IIT-CDIP	Open
GPT-4o	∼200B	Text+Vision+Audio	Web+Images+Audio	Closed
Gemini 1.5	175B	Text+Vision+Audio	Web+Multimodal	Closed
InternVL2	8B	Text+Vision	Documents, Medical	Open
QwenVL2	72B	Text+Vision+Video	Web, OCR, Video	Open
Idefics2	8B	Text+Vision	Web, Documents	Open

B.1 Warmer Variants Details

RoBERTa is a self-supervised text-only language model trained on a large corpus (Liu, 2019), including BookCorpus, English Wikipedia, CommonCrawl News, OpenWebText, and Stories datasets. RoBERTa removes the next-sentence prediction (NSP) objective and uses dynamic masking, larger batch sizes, and longer sequences.

LiLT (Language-independent Layout Transformer) extends pretrained text encoders with a lightweight layout encoder (Wang et al., 2022a). It is pretrained on the IIT-CDIP scanned document corpus. LiLT features a dual-stream architecture to separately encode text and layout (bounding box) information, with Bi-directional Attention Complementation (BiACM) to enhance cross-modal alignment.

LayoutLMv3 is a multimodal Transformer that jointly encodes text, layout, and image information (Huang et al., 2022). It is pretrained on the IIT-CDIP corpus and synthetic document data, using masked language modeling (MLM), masked image modeling (MIM), and word-patch alignment (WPA) tasks.

B.2 Large Vision-Language Models details

B.2.1 Close Source Models

GPT-4o is a multimodal model capable of processing text, images, and audio, with an estimated parameter count of hundreds of billions to 1 trillion (OpenAI, 2024). Trained on web-scale text, images, and audio, GPT-4o features native multimodal reasoning, multilingual support, and high-speed inference.

Gemini 1.5 Pro is a mid-size multimodal model with a Mixture-of-Experts (MoE) architecture, trained on a vast multimodal corpus with a focus on long-context tasks up to 1 million tokens (Team et al., 2024): .

B.2.2 Open Source Models

InternVL2 combines a vision Transformer and a language model (Chen et al., 2024). It is pretrained on 5M curated multimodal samples, including documents, forms, scientific charts, and medical images. InternVL2 ranges from 1B to 108B parameters and is pretrained on curated multimodal data, including documents, forms, scientific charts, and medical images. It achieves competitive results on specific document-centric tasks, such as DocVQA.

QwenVL2 is trained on 1.4T tokens, including image-text pairs, OCR data, video, and interleaved documents (Wang et al., 2024). With innovations like Naive Dynamic Resolution and Multimodal RoPE, QwenVL2 achieves competitive performance on multimodal benchmarks, establishing itself as a leading open-source option.

Idefics2 combines a Mistral-7B language model with a SigLIP vision encoder (Laurençon et al., 2024). Trained on interleaved web documents, captions, OCR data, and diagram-text mappings, it supports arbitrary sequences of text and images. Despite its smaller size, it achieves performance comparable to that of 30B+ models.

C Detailed Prompts

We list all the prompts used in this paper for synthetic data generation in Table S3 and MLLM zero-shot testing in Table S4.

Table S3: Synthetic Data Generator Prompt Example

Module	**Prompt Description**	**Prompt Template**
User-Input Verification	Checks whether the target information was entered by the user or is part of the form template.	`Based on the provided Context {} from the target form and the form image itself, check if the target information itself (do not consider the context) {} was entered by the form user (not part of the form template). Only output "Yes" if the {} is exactly provided by the user, not from the form template, and do not consider context information. The response should follow the format below: "Response": "Yes/No"`
Semantic Question Generation	Generates a short human-asked question where the answer exactly matches the target.	`Based on the above context {} and target document image, generate a human-asked SHORT question (output question only) of which answer is exactly the same as {}`
Answer Verification	Verifies whether the given target could be the expected answer to the given question.	`Ignore the context information and domain knowledge (e.g., FAX NUMBER). Just consider whether {} could be the expected answer to the question {}. Output format: {'Response': 'Yes/No', 'Explanation': 'xxx'}.`
Layout-Aware Question Reformulation	Reformulates a question into a short question about the location of the answer in the document.	`Change the question {} to a very short question about finding the position of the answer from the input document image. For example, where is the answer to xx located?`

Table S4: Summary of Inference Prompt Functions and Their Templates

Module	**Prompt Description**	**Prompt Template**

Text-Image QA without Tips	Generates a response to a question based on an image and text context, without any additional Tips.	`Above is the context {} of the target {}. Please answer the question {} based on the context and image. The output format must strictly follow:`
		`Answer: xxx`

Text-Image QA with One Tip	Generates a response to a question based on an image and text context, with a single Tip.	`The above is the context {} of the target {}. This is a Tip: {} (which may not be correct). Please answer the question {} based on the context and image. The output format must strictly follow:`
		`Answer: xxx`

Text-Image QA with Multiple Tips	Generates a response to a question based on an image and text context, with multiple ranked Tips.	`The above is the context {} of the target {}. These are the Tips (which may not be correct):`
		`Please answer the question {} based on the context and image. The output format must strictly follow:`
		`Answer: xxx`

Text-Image QA with Bounding Boxes (No Tips)	Generates a response to a question based on an image, text context, and bounding box overlays, without any additional Tips.	`Above is the context {} of the target {} document,`
		`Please answer the question {},`
		`Based on the context and image,`
		`The output format strictly follows:`
		`Answer: xxx`

Text-Image QA with Bounding Boxes (One Tip)	Generates a response to a question based on an image, text context, and bounding box overlays, with a single Tip.	`The above is the context {} of the target {} document.`
		`This is a Tip: {} (which may not be correct).`
		`Please answer the question {},`
		`Based on the context and image,`
		`The output format strictly follows:`
		`Answer: xxx`

Text-Image QA with Bounding Boxes (Multiple Tips)	Generates a response to a question based on an image, text context, and bounding box overlays, with multiple ranked Tips.	`The above is the context {} of the target {} document.`
		`These are Tips: {}, (which may not be correct.)`
		`Please answer the question {},`
		`Based on the context and images,`
		`The output format strictly follows:`
		`Answer: xxx`

D Computational Cost

D.1 Warmer Tuning Cost

Table S5 presents the training and inference resource consumption across five benchmark datasets with a consistent batch size of 16. The GPU memory usage remains within a reasonable range (approximately 25.5GB–28GB), demonstrating the framework's efficiency and scalability on standard hardware. The structural and semantic training times per epoch are well-balanced, typically ranging from 2 to 8 minutes, depending on dataset complexity. Notably, the inference time remains minimal—under 2.5 minutes for all datasets—highlighting the framework's practical deployment potential. These results indicate that the proposed framework achieves a favorable trade-off between training cost and performance, making it suitable for both research and real-world applications.

Table S5: Per-epoch GPU consumption and time cost across different datasets with a fixed batch size of 16. The times correspond to the most effective training configurations: 2 epochs for structural adaptation and 10 epochs for semantic adaptation.

Dataset	Batch Size	GPU Consumption	Structural Time (1 Epoch)	Semantic Time (1 Epoch)	Inference Time
FormNLU-P	16	27983.4M	00:03:46	00:03:08	00:01:10
FormNLU-H	16	25736.0M	00:03:58	00:03:01	00:01:02
CORD	16	26174.5M	00:04:30	00:04:02	00:02:01
EPHOIE	16	27993.1M	00:06:01	00:03:12	00:01:14
FUNSD	16	25566.2M	00:08:10	00:02:01	00:00:59

D.2 SynDoc Time Latency

The results in Table S6 demonstrate that SynDoc's recursive inference mechanism introduces only a modest increase in runtime while delivering consistent accuracy gains across datasets. Although the best-performing configuration requires slightly longer inference times—ranging from approximately 1.5× to 2× the latency of the vanilla setup—the improvement in ANLS is both stable and meaningful, particularly on FormNLU-P (+4.2 ANLS) and CORD (+0.8 ANLS). Importantly, most samples complete after a single iteration, keeping the overhead manageable. This lightweight inference cost stands in sharp contrast to traditional document KIE pipelines that rely on extensive manual annotation or expensive LLM/MLLM fine-tuning. By shifting complexity from heavy training to efficient inference, SynDoc provides a resource-efficient strategy that avoids knowledge leakage and tuning conflicts while achieving stronger zero-shot extraction performance.

Table S6: Comparison of runtime (mm:ss) and ANLS across configurations.

Config	**FormNLU-P**		**FormNLU-H**		**CORD**		**EPHOIE**	
	Time	ANLS	Time	ANLS	Time	ANLS	Time	ANLS
Vanilla	15:24	76.09	17:22	66.86	06:26	84.35	35:25	81.82
Best Performed	30:47	80.29	31:17	67.73	11:27	85.19	84:17	82.15

E Additional Evaluation Results

E.1 Various Prompt Modality Performance

We present results from various prompting methods applied to baseline MLLMs and the Gemini-based SynDoc framework (Table S7). The findings indicate that multimodal prompting, which integrates OCR-extracted textual context with document images, generally enhances performance. However, the OCR Challenging dataset exhibits difficulties in some instances. For image-only prompting, some open-source models perform relatively poorly. Consequently, our SynDoc framework adopts the Image + Text context prompt as the primary approach for overall evaluation and ablation studies.

Table S7: Performance comparison of various models on different datasets.

Models	Prompt	Formnlu-P	Formnlu-H	CORD	Ephoie	Funsd
InternVL2	Context-only	59.65	7.16	44.00	54.39	53.48
Qwen2-VL		72.12	10.04	65.20	61.59	68.87
Idefics2		28.52	3.33	4.33	8.90	21.98
GPT-4o		71.64	1.45	69.88	59.78	68.71
Gemini		70.88	5.91	71.53	59.94	68.21
InternVL2	Image-only	68.28	48.85	62.86	63.92	74.85
Qwen2-VL		79.17	55.35	75.85	83.79	83.06
Idefics2		46.97	35.64	51.54	2.97	58.48
GPT-4o		74.81	56.51	77.63	62.23	80.32
Gemini		79.78	66.29	81.48	76.07	83.79
InternVL2	Context + Image	66.56	45.47	66.84	68.92	74.95
Qwen2-VL		79.71	55.33	79.12	83.35	82.77
Idefics2		57.54	33.31	54.45	15.22	62.11
GPT-4o		76.16	56.49	79.05	79.40	80.05
Gemini		76.09	66.86	84.35	81.82	83.56
SynDoc	Context + Image	81.91	68.02	85.19	82.15	83.02
SynDoc	Context + Image + bbox	80.93	68.13	85.40	82.08	83.87

E.2 Various Prompting and RAG Method Performance

To further validate the effectiveness of SynDoc, we conducted comprehensive comparisons against multiple prompting-based reasoning approaches (Chain-of-Thought, Self-Consistency, Reflexion) as well as sparse and dense RAG baselines. For prompting methods, Chain-of-Thought responses were generated using explicit reasoning instructions, while Self-Consistency and Reflexion were executed with a maximum of five iterative reasoning steps. All of these methods operate solely on the input context and the implicit perceptual and world knowledge of the MLLM, without any external adaptation. Across all datasets, SynDoc achieves consistently higher accuracy while requiring substantially less inference time compared to these iterative reasoning strategies, highlighting the efficiency of its recursive retrieval–generation interaction.

We additionally benchmarked traditional RAG pipelines using both sparse (TF-IDF, BM25) and dense retrievers-based on Sentence-BERT (Top-5 retrieval). These methods typically introduce noisy or irrelevant passages into the context window, which in turn degrades MLLM performance. This trend underscores a key advantage of SynDoc: the warmer, trained using synthetic structural and semantic adaptation signals, retrieves fine-grained and domain-grounded cues rather than raw passages. As a result, SynDoc mitigate the noise amplification commonly observed in classical RAG systems and provides stable, high-quality guidance to the MLLM throughout inference.

E.3 More Warmer Ablation Studies

The results in Table S9 show that the joint-grained framework generally outperforms both the fine-grained and coarse-grained variants across most datasets, demonstrating its stronger adaptation capability when semantic and structural cues are integrated. While the fine-grained span-based QA head performs poorly on all benchmarks due to its limited ability to generalize from synthetic annotations, the coarse-grained entity retriever provides a substantial improvement by leveraging more stable structural patterns in documents. The joint configuration further enhances performance on

Table S8: Comparison of ANLS and Runtime (mm:ss) Across Various Prompting and Retrieval Methods

Model	FormNLU-P (F-P)		FormNLU-H (F-H)		CORD		EPHOIE		FUNSD	
	ANLS	Time	ANLS	Time	ANLS	Time	ANLS	Time	ANLS	Time
CoT	77.78	15:11	65.67	17:48	84.56	06:23	81.17	35:25	83.12	10:24
Self-Consistency	75.78	44:59	67.56	72:51	83.99	33:11	81.52	174:11	82.98	60:11
Reflexion	78.43	45:21	68.19	75:13	85.11	40:32	81.23	191:45	84.01	56:25
TF-IDF	75.24	15:02	64.12	16:30	83.22	06:01	81.01	33:11	82.43	10:03
BM25	75.45	16:34	64.72	17:21	83.48	06:32	80.82	37:32	83.00	10:21
Dense	74.25	15:43	65.95	17:44	83.51	06:22	81.74	34:24	81.77	09:22
SynDoc	**80.29**	30:47	**67.73**	31:17	**85.19**	11:27	**82.15**	84:17	**83.87**	21:23

Table S9: Impact of Grainularity on Domain Adaptation Performance (ANLS).

Granularity	FormNLU-P	FormNLU-H	CORD	EPHOIE
Fine-grained Span-based QA Head	38.72	15.50	47.21	20.52
Coarse-grained Entity Retrieving Head	65.35	25.55	63.17	29.74
Joint (Fine + Coarse)	**66.19**	**28.29**	**66.25**	27.16

FormNLU-P, FormNLU-H, and CORD, confirming that combining granularities enables richer and more complementary document understanding. The only exception is EPHOIE, where coarse-grained retrieval slightly surpasses the joint model—likely a result of limited Chinese-text modelling capacity in the LayoutLMv3-Chinese backbone, which restricts fine-grained semantic alignment. Overall, the trend validates that synthetic semantic/structural adaptation is most effective when both grain levels are jointly optimized.

E.4 Effectiveness of Recursive Inference.

Recursive inference is introduced to enhance both Warmer retrieval and the quality of MLLM-generated answers. Table S10 shows that models exhibit improved performance when more than one iteration is conducted. This demonstrates that Warmer and the LLM generator can mutually reinforce each other, enabling the model to generate more accurate final predictions. Additionally, we observed that open-source models (InternVL, QWenVL) typically require more iterations to reach peak performance, while the closed-source Gemini often achieves its best results with fewer iterations. Moreover, datasets that present OCR challenges (F-H and Ephoie) benefit from additional iterations, with all models requiring at least two iterations for optimal performance.

Table S10: Performance trends of iterative tuning. Int: InternVL2; QW: QWenVL2; Gemi: Gemini.

Iter.	F-P			F-H			CORD			EPHOIE		
	Int	Qw	Gemi	Int	QW	Gemi	Int	QW	Gemi	Int	QW	Gemi
Vani.	66.56	78.05	76.09	45.47	43.65	66.86	66.84	77.86	84.35	68.92	70.36	81.82
Iter 1	68.09	76.53	**80.29**	46.81	44.43	67.73	**68.80**	76.93	**85.19**	68.54	75.03	81.80
Iter 2	**70.12**	77.22	80.17	46.17	**45.27**	67.60	67.89	76.70	84.67	69.49	**75.55**	**81.91**
Iter 3	68.54	76.75	80.15	**47.23**	44.50	67.32	67.29	76.93	84.65	**70.24**	75.44	81.71
Iter 4	68.28	**77.27**	79.88	45.54	45.26	**67.63**	66.84	76.70	84.39	68.99	75.55	82.15
Iter 5	70.21	76.75	80.06	44.86	44.51	67.63	67.28	**76.93**	84.40	70.07	75.44	81.86

E.5 More Detailed Experimental Results

We provide detailed experimental results for different configurations of MLLM inference, from Table S11 to Table S13.

Table S11: Performance comparison across iterations for different models on the CORD, Printed, Handwritten, Ephoie, and FUNSD dataset with Top-1 warmer retrieved entity.

Model	**Baseline**		**Iteration 1**		**Iteration 2**		**Iteration 3**		**Iteration 4**		**Iteration 5**	
	Warmer	LLM	Warmer	LLM	Warmer	LLM	Warmer	LLM	Warmer	LLM	Warmer	LLM
CORD												
InternVL	67.26	66.84	63.38	68.80	57.74	67.89	58.50	67.29	59.70	66.84	57.82	67.28
QWenVL (2B)	67.26	12.17	63.38	16.36	59.75	16.75	59.86	16.43	59.75	16.75	59.86	16.43
QWenVL (7B)	67.26	77.86	63.38	76.93	59.89	76.70	59.64	76.93	59.89	76.70	59.64	76.93
QWenVL (72B)	67.26	79.12	63.38	78.02	59.98	77.96	60.30	77.81	59.98	77.96	60.30	77.81
Gemini	67.26	84.35	63.37	85.19	64.15	84.67	64.32	84.65	64.32	84.39	64.04	84.40
Printed												
InternVL	66.19	66.56	73.57	68.09	68.65	70.12	70.32	68.54	69.20	68.28	69.19	70.21
QWenVL (2B)	66.19	44.85	73.57	50.34	61.63	50.45	61.82	50.52	61.76	50.48	61.84	50.54
QWenVL (7B)	66.19	78.05	73.57	76.53	72.52	77.22	73.18	76.75	72.61	77.27	73.18	76.75
QWenVL (72B)	66.19	79.71	73.57	81.21	74.41	81.42	74.54	81.20	74.58	81.42	74.54	81.20
Gemini	66.19	76.09	73.57	80.29	73.76	80.17	73.72	80.15	73.76	79.88	73.60	80.06
Handwritten												
InternVL	31.64	45.47	38.11	46.81	32.29	46.17	32.70	47.23	32.06	45.54	32.76	44.86
QWenVL (2B)	31.64	14.56	38.11	19.21	24.95	19.33	25.45	19.19	25.02	19.36	25.44	19.20
QWenVL (7B)	31.64	43.65	38.11	44.43	34.51	45.27	35.25	44.50	34.83	45.26	35.26	44.51
QWenVL (72B)	31.64	55.33	38.11	58.33	38.37	58.40	38.33	58.37	38.48	58.58	38.36	58.37
Gemini	31.64	66.86	38.11	67.73	38.79	67.60	39.15	67.32	38.84	67.63	38.92	67.63
Ephoie												
InternVL	27.16	68.92	27.98	68.54	25.78	69.49	25.94	70.24	26.00	68.99	25.96	70.07
QWenVL (2B)	27.16	46.13	27.98	36.51	27.10	37.00	26.78	36.39	27.10	36.97	26.78	36.39
QWenVL (7B)	27.16	70.36	27.98	75.03	26.79	75.55	26.76	75.44	26.79	75.55	26.76	75.44
QWenVL (72B)	27.16	83.35	27.98	81.95	26.38	82.08	26.51	82.06	26.38	82.08	26.51	82.06
Gemini	27.16	81.82	27.98	81.80	25.94	81.91	26.03	81.71	25.94	82.15	26.12	81.86
FUNSD												
InternVL	61.24	74.95	59.64	73.18	58.30	72.13	58.44	73.41	58.97	73.57	58.98	73.12
QWenVL	61.24	79.12	61.94	74.84	60.03	75.73	60.92	74.57	59.93	75.73	60.92	74.57
Gemini	61.24	83.56	59.17	82.77	59.77	83.02	60.06	82.38	59.54	82.91	60.11	82.36

Table S12: Top-3 Warmer Retrieved Entity Performance comparison across iterations for different models on the CORD, Printed, Handwritten, and Ephoie dataset.

Model	**Baseline**		**Iteration 1**		**Iteration 2**		**Iteration 3**		**Iteration 4**		**Iteration 5**	
	Warmer	LLM	Warmer	LLM	Warmer	LLM	Warmer	LLM	Warmer	LLM	Warmer	LLM
CORD												
InternVL	67.26	66.84	63.38	61.61	60.19	65.31	53.73	64.75	53.52	61.70	54.06	62.22
QWenVL	67.26	77.86	63.38	78.16	59.65	77.96	59.34	78.12	59.65	77.96	59.34	78.12
Gemini	67.26	84.35	63.38	83.46	63.79	82.34	63.42	83.07	63.42	83.07	63.69	83.00
Printed												
InternVL	66.19	66.56	73.56	65.91	67.70	67.85	67.55	67.12	68.53	66.21	66.92	66.38
QWenVL	66.19	78.05	73.57	77.08	72.93	76.60	72.81	76.63	72.53	76.72	72.80	76.67
Gemini	66.19	76.09	73.99	81.60	74.12	81.91	74.30	81.63	74.01	81.58	74.28	81.46
Handwritten												
InternVL	31.64	45.47	38.11	43.48	32.64	43.24	30.92	42.02	31.75	43.15	31.93	43.52
QWenVL	31.64	43.65	38.11	42.03	33.65	43.37	33.68	41.66	32.60	42.62	33.28	41.55
Gemini	31.64	66.86	38.11	66.82	39.35	67.68	39.48	67.12	39.15	66.80	38.79	67.49
Ephoie												
InternVL	27.16	68.92	27.98	70.29	26.00	69.04	26.08	69.35	26.17	68.15	26.30	69.41
QWenVL	27.16	70.36	27.98	73.91	26.36	74.29	26.68	74.18	26.28	74.29	26.68	74.18
Gemini	27.16	81.82	27.98	81.18	26.23	81.13	26.25	81.16	26.27	81.43	26.10	81.32

Table S13: Top-5 Performance comparison across iterations for different models on the CORD, Printed, Handwritten, and Ephoie dataset.

Model	**Baseline**		**Iteration 1**		**Iteration 2**		**Iteration 3**		**Iteration 4**		**Iteration 5**	
	Warmer	LLM	Warmer	LLM	Warmer	LLM	Warmer	LLM	Warmer	LLM	Warmer	LLM
CORD												
InternVL	67.26	66.84	63.37	64.25	57.02	63.21	54.63	68.18	55.93	66.76	57.87	65.13
QWenVL	67.26	77.86	63.38	78.20	59.54	77.49	58.91	78.44	60.08	77.53	58.91	78.16
Gemini	67.26	84.35	63.38	84.57	63.79	82.85	63.99	83.37	63.79	82.77	63.79	83.39
Printed												
InternVL	66.19	66.56	73.57	66.88	69.19	66.17	67.46	65.23	65.67	65.67	66.27	66.27
QWenVL	66.19	78.05	73.57	76.35	72.22	77.01	72.66	76.67	72.34	77.27	72.70	76.21
Gemini	66.19	76.09	73.58	80.10	73.35	80.35	73.70	80.20	73.40	80.36	73.54	80.08
Handwritten												
InternVL	31.64	45.47	38.11	43.82	32.79	44.13	33.66	43.78	31.87	41.55	32.11	43.22
QWenVL	31.64	43.65	38.11	40.12	32.51	41.97	33.13	40.18	32.26	41.75	32.99	39.78
Gemini	31.64	66.86	38.11	66.90	39.05	67.33	39.06	67.51	38.99	67.01	39.11	68.02
Ephoie												
InternVL	27.16	68.92	27.98	68.88	26.18	68.66	25.93	67.90	26.06	69.61	25.87	69.77
QWenVL	27.16	70.36	27.98	74.32	26.32	74.32	26.56	74.35	26.32	74.34	26.67	74.24
Gemini	27.16	81.82	27.98	81.33	26.35	81.18	26.31	81.58	26.37	81.23	26.28	81.45

F ADDITIONALY CASE STUDIES

Figures S1 and S2 present qualitative case studies from the CORD and Ephoie datasets, respectively, highlighting the complementary strengths of the MLLM-based self-correction pipeline and the Top-K retrieval. In Figure S1, the MLLM initially predicts "24,000", and the Warmer module retrieves a noisy string "Qty=4.00240.000". Despite the noise, the final MLLM module correctly interprets the answer as "4", demonstrating its robustness to OCR errors and its ability to reason over imperfectly retrieved content. In Figure S2, a query about a student's name is given, where the initial MLLM output is incorrect. However, the Warmer module retrieves relevant entities and ranks the correct answer within the Top-3, enabling the final MLLM stage to recover the accurate result. These examples collectively demonstrate the pipeline's effectiveness in overcoming early-stage retrieval errors and OCR-related noise in complex document QA tasks.

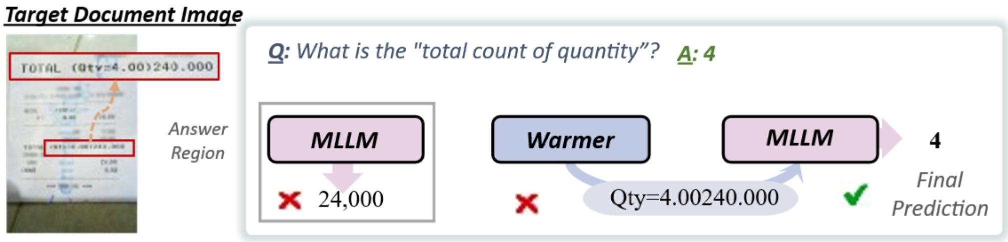

Figure S1: Qualitative case studies about the CORD dataset for demonstrating the effectiveness of Warmer in retrieving the content and the MLLM self-correction ability for OCR errors.

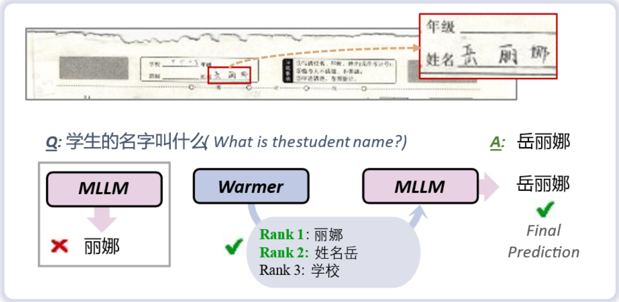

Figure S2: Qualitative case studies about the Ephoie dataset for demonstrating the effectiveness of Top-K.

G LLM USAGE

Large Language Models (LLMs) were used to aid in the writing and polishing of the manuscript. Specifically, we used an LLM to refine the language, improve readability, and ensure clarity across various sections of the paper. The model helped with tasks such as sentence rephrasing, grammar checking, and enhancing the overall flow of the text.

It is important to note that the LLM was not involved in the ideation, research methodology, or experimental design. All research concepts, ideas, and analyses were developed and conducted by the authors. The contributions of the LLM focused solely on improving the paper's linguistic quality, with no involvement in the scientific content or data analysis.

The authors take full responsibility for the content of the manuscript, including any text generated or polished by the LLM. We have ensured that the LLM-generated text adheres to ethical guidelines and does not contribute to plagiarism or scientific misconduct.